Sea State Uncertainty-aware Monitoring of Underwater Mooring Systems Using Domain-Adapted Deep Learning Techniques

Yixuan Liu[a], Shangyan Zou[c], Xin Ye[d], and Kai Zhou[*a,b]

[a]Department of Civil and Environmental Engineering, The Hong Kong Polytechnic University, Hong Kong, China
[b]Research Institute for Sustainable Urban Development, The Hong Kong Polytechnic University, Hong Kong, China
[c]Department of Mechanical and Aerospace Engineering, Michigan Technological University, MI, USA
[d]College of Civil Engineering and Architecture, Wenzhou University, Zhejiang, China
[*]cee-kai.zhou@polyu.edu.hk

ABSTRACT

Underwater mooring systems are essential for marine infrastructure safety but face stiffness reduction and potential failure due to long-term environmental loads like waves and currents, requiring timely and accurate health monitoring. Data-driven deep learning techniques, which identify mooring system health from dynamic responses, offer more efficient and cost-effective solutions compared to traditional methods. However, the high complexity and uncertainty of the sea state pose challenges for effective monitoring tasks utilizing general deep learning models. While ocean wave spectra are often considered invariant over relatively short time scales, the exact time series of free sea surface elevation remains inherently unpredictable, which interferes with the health-related features to degrade the monitoring reliability and accuracy. To address this challenge, this study integrates domain adaptation techniques into deep learning models to mitigate distribution discrepancies and enhance the generalization of these models. Case studies demonstrate that the model exhibits significantly improved generalization ability, showing great potential for managing mooring system monitoring in practical applications.

Keywords: underwater mooring systems; health monitoring; deep learning; domain adaptation.

1. INTRODUCTION

1.1 Background

Mooring systems are essential for ensuring the stability and safety of offshore floating structures such as floating wind turbines and offshore oil platforms. Exposed to harsh marine conditions, these systems face dynamic loads from waves and currents, leading to stiffness degradation, structural fatigue, and potential failure.[1] Such failures threaten operational safety, environmental sustainability, and the economic viability of offshore projects.[2]As demand for renewable energy grows, floating wind turbines are increasingly deployed in deeper waters to access stronger and more consistent winds. The operational efficiency of these structures heavily depends on the reliability of their mooring systems. Traditional monitoring of marine structures relies on labor-intensive visual inspections and physical measurements. While these methods are effective in controlled environments, they are time-consuming, costly, and impractical for large-scale offshore infrastructure operating in harsh marine conditions.

In recent years, advancements in data-driven technologies, particularly deep learning, have provided new directions for structural monitoring. These methods, which combine dynamic response data such as six degrees of freedom (6-DOF) platform motions with advanced machine learning algorithms, show significant potential in identifying structural damage.[3,4] Statistical wave spectrum parameters, such as significant wave height and peak period, are commonly used to model the impact of ocean waves on platform motions. While these parameters

provide a useful statistical description of wave energy distribution, they are insufficient to fully describe the temporal evolution of ocean surface elevations.[5] Most existing response-based structural monitoring methods simplify wave conditions as deterministic and consistent under a given spectrum, neglecting the inherent randomness of ocean waves. Consequently, these methods often struggle to generalize effectively in real-world marine environments.

1.2 Previous Work and Limitations

In our prior study,[6] we focused on monitoring stiffness reduction in mooring systems of OC4 semi-submersible floating platform under single sea state conditions. This approach utilized a high-fidelity finite element model to simulate platform dynamic responses for various combinations of mooring line stiffness. By using convolutional neural networks (CNNs), the study demonstrated the feasibility of applying data-driven techniques to structural health monitoring. The results showed that CNNs could effectively identify stiffness reduction patterns, providing a data-driven approach to damage detection in marine environments.

However, the study assumed that sea states were deterministic and consistent for given spectral parameters, neglecting the inherent randomness of ocean waves. This limitation becomes evident when extending the method to scenarios with stochastic variability wave, as the models struggled to generalize to real-world marine environments. Addressing these challenges requires datasets that explicitly capture wave randomness and advanced learning frameworks capable of handling such variability. This study designs unique datasets and models that explicitly capture wave randomness, aiming to improve generalization and robustness in structural health monitoring.

2. DATASET AND BASELINE MODEL

2.1 Dataset Preparation

To address the limitations identified in previous work, two datasets were designed to capture wave-induced randomness and stiffness reduction in platform dynamics. These datasets form the foundation for developing models capable of handling stochastic variability in real-world sea states. The OC4 semi-submersible platform was simulated to generate dynamic response data under varying sea states, following the approach in our previous work.[6] Typical South China Sea wave conditions[7,8] were selected as environmental excitation, with only wave effects considered for simplicity. As shown in Figure 1.

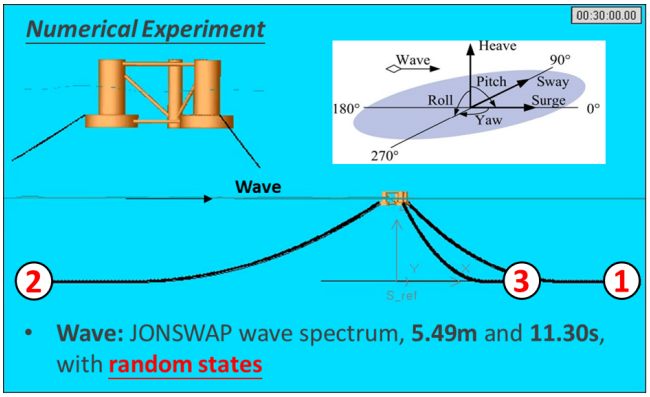

Figure 1. Illustration of the OC4 semi-submersible platform under JONSWAP wave spectrum conditions. The platform responses include six degrees of freedom (6-DOF): surge, sway, heave, roll, pitch, and yaw. Random wave states with significant wave height of 5.49 m and peak period of 11.30 s were used for simulation.

Two datasets, Dataset 1 and Dataset 2, were generated to evaluate mooring system health under varying sea state conditions. Dataset 1 was created using uniform sampling, including 1,000 stiffness combinations to capture diverse damage scenarios. To incorporate wave randomness, 10 random seeds were applied per stiffness combination, resulting in 10,000 samples for training. Dataset 2, generated using Latin Hypercube Sampling

(LHS), included 100 stiffness combinations paired with 100 random sea states. This smaller dataset, with 100 samples, was designed to evaluate the ability of the model to generalize to unseen real-world environments.

Each dataset sample included time-series data of six degrees of freedom (6-DOF) dynamic responses, reflecting key mechanical behaviors under varying wave conditions and stiffness scenarios. The responses were generated for 3600 seconds at a sampling rate of 1 Hz, with the first 1100 seconds removed to eliminate the influence of transient responses on the results. Power Spectral Density (PSD) was computed to capture frequency-domain characteristics, complementing the time-domain features. Welch's method was employed, averaging overlapping signal segments to provide a robust, noise-resistant estimate of energy distribution across frequencies.[9]

2.2 Baseline Model: ResNet-18

ResNet-18, a residual convolutional neural network introduced by He et al.,[10] was selected as the baseline model for evaluating mooring system health monitoring under varying wave conditions. Residual networks address the vanishing gradient problem using shortcut connections or "residual blocks," allowing efficient learning of complex transformations. As a lightweight architecture with 18 layers, ResNet-18 is well-suited for extracting patterns from high-dimensional time-series data.

In this study, ResNet-18 was adapted to process one-dimensional sequential features, treating six degrees of freedom (6-DOF) dynamic responses as multi-channel inputs. Both time-domain and frequency-domain data were fed into the network to capture features associated with stiffness reduction labels. The model was trained on Dataset 1 (10,000 samples) and tested on Dataset 2 (100 samples). A validation set drawn from Dataset 1 revealed near-perfect R^2 scores across the three mooring lines, as depicted in Figure 2. Each output corresponds to the stiffness reduction of a specific mooring line, with the second output representing the mooring line facing incoming waves. These results demonstrate the model's ability to predict stiffness reductions under controlled conditions.

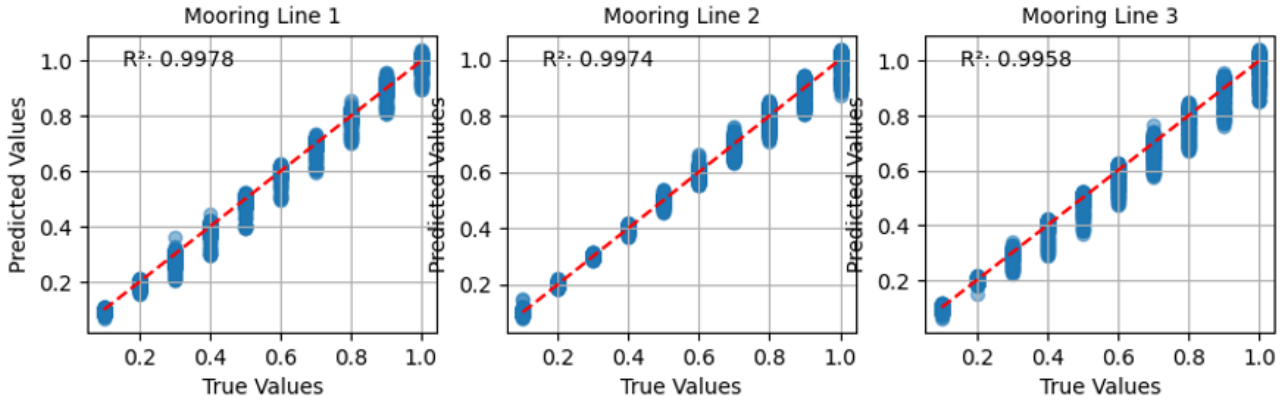

Figure 2. Predicted versus true stiffness levels for mooring lines across three mooring lines. Each subfigure represents the stiffness level of a specific mooring line: (a) Mooring Line 1, (b) Mooring Line 2, and (c) Mooring Line 3. The stiffness level ranges from 1 (no damage) to 0 (fully damaged).

Despite its strong performance on Dataset 1, ResNet-18 struggles to generalize to the stochastic sea conditions represented in Dataset 2. As shown in Figure 3 (Left), training and validation loss curves indicate effective convergence, showing that ResNet-18 successfully captures patterns in the training data. Figure 3 (Right) illustrates significant variability in R^2 scores across the three mooring lines under the stochastic conditions of Dataset 2. While the predictions for two mooring lines (Outputs 1 and 3) achieve acceptable exhibit negative R^2 values. This contrast highlights the model's difficulty in adapting to the inherent randomness and variability of real-world marine environments. Addressing this limitation is essential for improving the robustness of health monitoring models under real-world conditions.

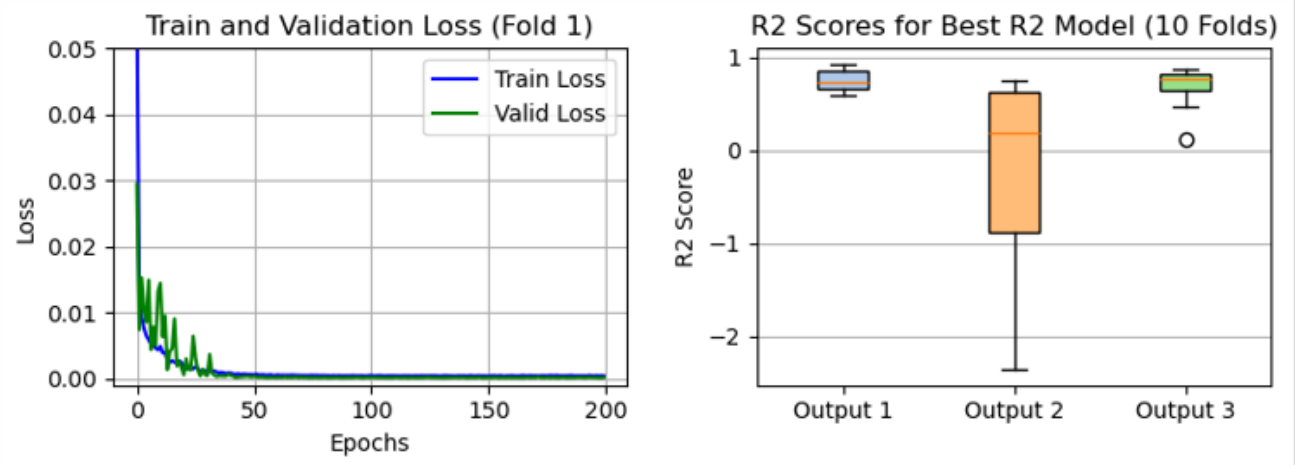

Figure 3. (Left) Training and validation loss curves for ResNet-18, showing effective convergence on Dataset 1. (Right) R^2 scores from 10-fold cross-validation models tested on Dataset 2, with significant variability across the three mooring lines.

3. ADVANCED MODELS

3.1 Domain-Adversarial Neural Network (DANN)

To address the poor generalization ability observed in ResNet-18 due to the significant differences in wave conditions between datasets, a Domain-Adversarial Neural Network (DANN) was introduced. Unlike traditional regression models that assume consistent feature distributions between training and testing data, DANN employs domain adaptation techniques to bridge the gap between the source domain (Dataset 1) and the target domain (Dataset 2).[11]

The feature extractor uses ResNet-18 layers to process six degrees of freedom (6-DOF) dynamic responses from both the time and frequency domains, extracting features relevant to stiffness prediction. The domain classifier distinguishes between the source and target domains, while the label predictor predicts stiffness reductions for each mooring line. To ensure domain-invariant feature extraction, a Gradient Reversal Layer (GRL) is integrated into the domain classifier, reversing the gradient direction during backpropagation. This alignment mechanism enables the feature extractor to generate consistent representations across domains, improving model generalization. The total loss function for the Domain-Adversarial Neural Network (DANN) combines the prediction loss and the domain classification loss, expressed as:

$$L_{\text{total}} = L_{\text{Predictor}} + \lambda L_{\text{domain}} \tag{1}$$

Here, $L_{\text{Predictor}}$ represents the supervised loss for stiffness prediction, while L_{domain} encourages alignment between the source and target domain feature distributions, and λ controls the balance between these two objectives.

In the implementation, Dataset 1 provides labeled data for supervised training, while Dataset 2, used as an unlabeled target domain, guides the model to align features across domains. As shown in Figure 4, the DANN Model demonstrates significant improvements over ResNet-18 on Dataset 2, with average R^2 increasing from negative values to approximately 0.83 for Output 2 (representing the mooring line facing the incoming waves). This indicates DANN's ability to adapt to more variable sea state conditions. However, some errors remain for Outputs 1 and 2, with R^2 values occasionally dropping to 0.5, reflecting challenges in capturing complex wave-induced dynamics.

Although DANN significantly improves prediction performance, certain challenges remain under highly uneven data distributions or more extreme sea state variations. The variability observed in the results suggests that the model, while improving domain alignment, may still struggle with balancing alignment and accuracy in specific conditions. This motivates the introduction of PAC-Regularized DANN, which further enhances the model by incorporating robustness measures against overfitting and excessive alignment.

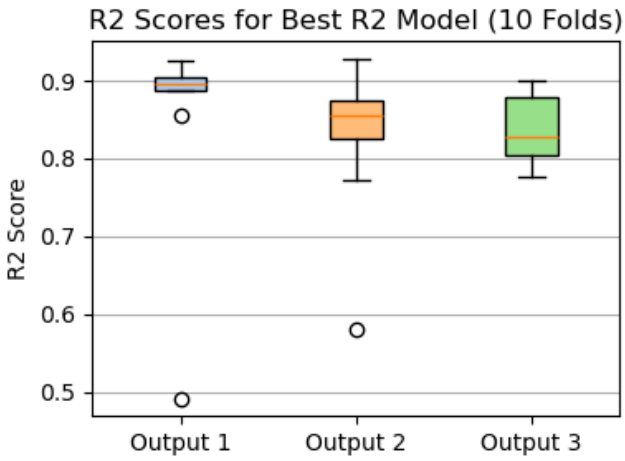

Figure 4. Performance of DANN on Dataset 2. Compared to ResNet-18, DANN achieves higher R^2 scores across all three mooring lines, demonstrating improved generalization to stochastic sea state conditions.

3.2 PAC-Regularized DANN

PAC-Regularized DANN builds on the DANN framework to further improve generalization under diverse sea state conditions. By incorporating PAC-Bayesian regularization,[12] this approach effectively balances domain alignment and model complexity, mitigating overfitting even under highly variable wave patterns.

In PAC-Regularized DANN, the feature extractor, domain classifier, and label predictor remain consistent with the DANN architecture. The key enhancement is the inclusion of a PAC-Bayesian term in the loss function, specifically the Kullback-Leibler (KL) divergence. This term ensures that the learned parameter distribution $Q(\theta)$ stays close to a prior distribution $P(\theta)$ (normally a Gaussian distribution), reducing overfitting and enhancing robustness against data imbalance and noise. The updated total loss function for PAC-Regularized DANN is expressed as:

$$L_{\text{total}} = L_{\text{Predictor}} + \lambda L_{\text{domain}} + KL(Q(\theta)\|P(\theta)) \tag{2}$$

Here, $KL(Q(\theta)\|P(\theta))$ penalizes deviations of the learned parameters from the prior distribution, ensuring that the model maintains a balance between complexity and generalization. The KL divergence is mathematically defined as:

$$KL(Q(\theta)\|P(\theta)) = \int Q(\theta) \log \frac{Q(\theta)}{P(\theta)} d\theta \tag{3}$$

This additional term encourages the model to avoid overfitting to specific training conditions by regularizing the parameter space, making it more robust when handling unseen wave-induced stochastic variations.

PAC-Regularized DANN was trained using Dataset 1 as the labeled source domain and Dataset 2 as the unlabeled target domain. Compared to DANN, this enhanced model demonstrates clear improvements, achieving higher and more consistent R^2 scores across all mooring lines (Figure 5). For he damage identification of the second mooring line, which performed the worst in the previous model, PAC-Regularized DANN significantly reduces prediction variability, minimizing extreme errors.

3.3 Performance Evaluation and Discussion

To evaluate the effectiveness of the proposed models, a comprehensive comparison of ResNet-18, DANN, and PAC-Regularized DANN was conducted. The evaluation focused on the models' ability to generalize under stochastic sea state conditions in Dataset 2. Key performance metrics included the average R^2 scores and their standard deviations across the three mooring lines are summarized in Figure 6 and Table 1.

ResNet-18, as the baseline model, displayed limited generalization, with inconsistent R^2 scores, especially for the second mooring line (Output 2). Negative R^2 values observed for Output 2 indicate its poor adaptability to variable sea conditions. High standard deviations further underline its lack of robustness.

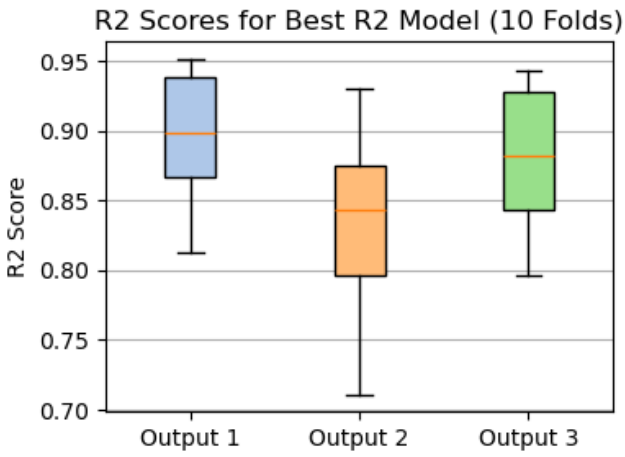

Figure 5. Performance of PAC-Regularized DANN on Dataset 2. Compared to DANN, this approach achieves consistently higher R^2 scores across all mooring lines, demonstrating improved robustness and generalization under diverse wave conditions.

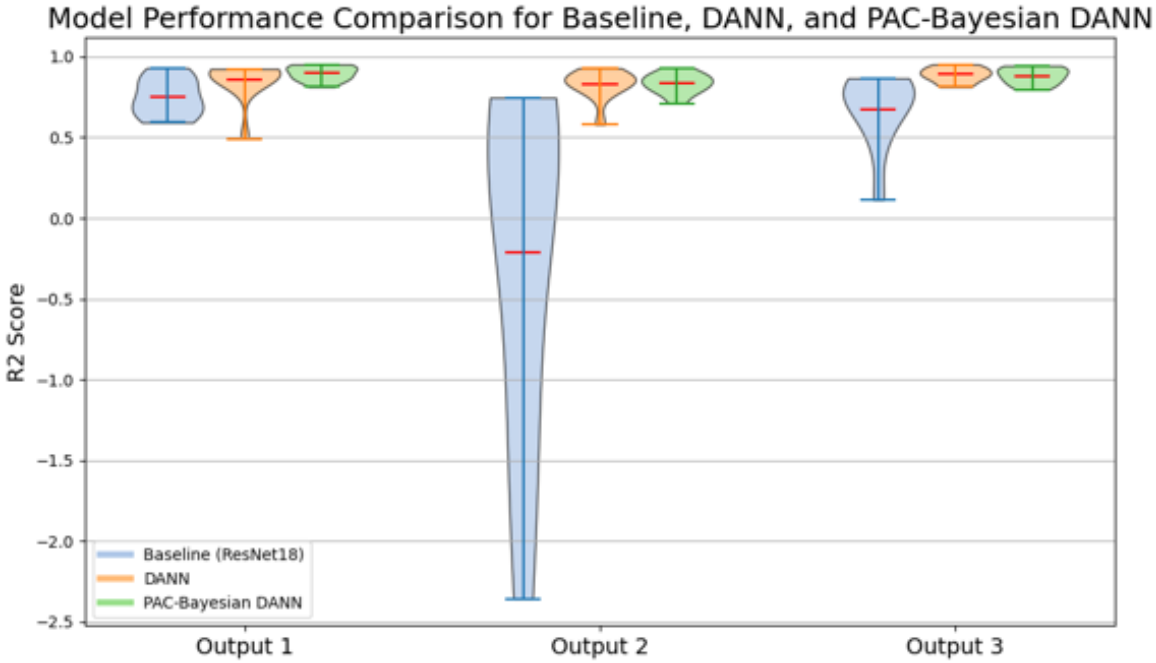

Figure 6. Model performance comparison for ResNet-18, DANN, and PAC-Regularized DANN. Violin plots show the R^2 score distributions across the three outputs (mooring lines) for each model. PAC-Regularized DANN demonstrates the best overall performance with reduced variability.

DANN showed clear improvements over ResNet-18 by integrating domain adaptation, and aligning feature distributions across training and testing datasets. R^2 scores improved across all outputs, with Output 2 achieving an average score of 0.83. However, relatively high standard deviations indicate lingering instability under complex wave conditions.

PAC-Regularized DANN overcame these challenges by incorporating the PAC-Bayesian regularization term, which constrained model complexity and improved prediction stability. It achieved the highest average R^2 scores, particularly excelling for Output 2, where the standard deviation was significantly reduced to 0.0638.

Table 1. Performance Metrics for ResNet-18, DANN, and PAC-Regularized DANN

Run	**Baseline (ResNet18)**			**DANN**			**PAC-Bayesian DANN**		
Output	**1**	**2**	**3**	**1**	**2**	**3**	**1**	**2**	**3**
1	0.6047	-1.5138	0.7681	0.9057	0.8759	0.8245	0.8485	0.8140	0.8232
2	0.9296	0.6144	0.8661	0.9250	0.8455	0.8927	0.9472	0.8710	0.8667
3	0.7094	0.7463	0.7846	0.4905	0.7722	0.7769	0.8131	0.7829	0.7960
4	0.8877	-1.1134	0.8293	0.8565	0.8742	0.8453	0.9141	0.7908	0.9302
5	0.8523	0.5072	0.8308	0.8913	0.8218	0.7914	0.8626	0.8433	0.8357
6	0.6956	0.6222	0.6120	0.9185	0.8669	0.8992	0.8819	0.7106	0.8820
7	0.5926	-0.1256	0.1127	0.8893	0.5797	0.7991	0.9521	0.8960	0.9224
8	0.6549	0.6939	0.7189	0.9008	0.8733	0.8170	0.8845	0.9308	0.9436
9	0.7430	-0.1972	0.7687	0.8871	0.8347	0.8303	0.9310	0.8438	0.8829
10	0.8275	-2.3597	0.4715	0.8998	0.9288	0.8895	0.9405	0.8767	0.9323
Average	**0.7497**	**-0.2126**	**0.6763**	**0.8565**	**0.8273**	**0.8366**	**0.8976**	**0.8360**	**0.8815**
STD	**0.1189**	**1.0935**	**0.2303**	**0.1300**	**0.0962**	**0.0441**	**0.0470**	**0.0638**	**0.0511**

This highlights the effectiveness of combining domain adaptation with regularization to enhance generalization and robustness.

In summary, the results demonstrate a clear progression from ResNet-18 to DANN and PAC-Regularized DANN, highlighting the benefits of domain adaptation and regularization. While DANN reduces domain gaps, PAC-Regularized DANN ensures greater robustness and consistency, providing a dependable approach for monitoring mooring system health under random and variable sea conditions.

4. CONCLUSION AND FUTURE WORK

This study presents a robust framework for predicting stiffness reduction in mooring systems under stochastic sea state conditions. Through intergrating? domain adaptation techniques, including DANN and PAC-Regularized DANN, the models demonstrated significant improvements over the baseline ResNet-18, effectively addressing the challenges posed by wave-induced randomness. Despite these achievements, the current models are limited to offline data analysis, as they are not yet capable of real-time monitoring. This limitation highlights the need for further development of computationally efficient algorithms and real-time data integration techniques. Furthermore, ongoing laboratory experiments are expected to validate the proposed framework using real-world data, moving beyond fully reliance on simulation models.

ACKNOWLEDGMENTS

This research is supported in part by NSF under grant CMMI – 2138522, and in part by research fund offered by the Research Institute for Sustainable Urban Development (RISUD) at The Hong Kong Polytechnic University.

REFERENCES

[1] Zhao, Y., Dong, S., and Jiang, F., "Reliability analysis of mooring lines for floating structures using ann-bn inference," *Proceedings of the Institution of Mechanical Engineers, Part M: Journal of Engineering for the Maritime Environment* **235**(1), 236–254 (2021).

[2] Weller, S., Johanning, L., Davies, P., and Banfield, S., "Synthetic mooring ropes for marine renewable energy applications," *Renewable energy* **83**, 1268–1278 (2015).

[3] Yang, Y., Bashir, M., Li, C., and Wang, J., "Investigation on mooring breakage effects of a 5 mw barge-type floating offshore wind turbine using f2a," *Ocean Engineering* **233**, 108887 (2021).

[4] Mao, Y., Zheng, M., Wang, T., and Duan, M., "A new mooring failure detection approach based on hybrid lstm-svm model for semi-submersible platform," *Ocean Engineering* **275**, 114161 (2023).

[5] Vandever, J. P., Siegel, E. M., Brubaker, J. M., and Friedrichs, C. T., "Influence of spectral width on wave height parameter estimates in coastal environments," *Journal of waterway, port, coastal, and ocean engineering* **134**(3), 187–194 (2008).

[6] Liu, Y., Zou, S., Gao, Q., and Zhou, K., "Physics-guided data-driven failure identification of underwater mooring systems in offshore infrastructures," in [*Health Monitoring of Structural and Biological Systems XVIII*], **12951**, 184–194, SPIE (2024).

[7] Liu, Z., Tianhui, F., and Chaonuclear, C., "Comparative hydrodynamic performance analysis of three typical semi-submersible floating wind turbine foundations," *China Offshore Platform* **36**(2), 1–10 (2021).

[8] Huang, X., Liu, Y., Liu, J., et al., "Mooring cable layout and fracture simulation analysis of deepcwind platform of offshore wind turbine," *Science Technology and Engineering* **23**(6), 2419–2427 (2023).

[9] Sakaris, C. S., Yang, Y., Bashir, M., Michailides, C., Wang, J., Sakellariou, J. S., and Li, C., "Structural health monitoring of tendons in a multibody floating offshore wind turbine under varying environmental and operating conditions," *Renewable Energy* **179**, 1897–1914 (2021).

[10] He, K., Zhang, X., Ren, S., and Sun, J., "Deep residual learning for image recognition," in [*Proceedings of the IEEE conference on computer vision and pattern recognition*], 770–778 (2016).

[11] Ganin, Y., Ustinova, E., Ajakan, H., Germain, P., Larochelle, H., Laviolette, F., March, M., and Lempitsky, V., "Domain-adversarial training of neural networks," *Journal of machine learning research* **17**(59), 1–35 (2016).

[12] Rothfuss, J., Fortuin, V., Josifoski, M., and Krause, A., "Pacoh: Bayes-optimal meta-learning with pac-guarantees," in [*International Conference on Machine Learning*], 9116–9126, PMLR (2021).